Three-dimensional speckle size in generalized optical systems with limiting apertures

Jennifer E. Ward,[1] Damien P. Kelly,[2] and John T. Sheridan[1,*]

[1]*School of Electrical, Electronic and Mechanical Engineering, UCD Communications and Optoelectronic Research Centre, SFI-Strategic Research Cluster in Solar Energy Conversion, College of Engineering, Mathematics and Physical Sciences, University College Dublin, Belfield, Dublin 4, Ireland*
[2]*Department of Computer Science, National University of Ireland, Maynooth, Ireland*
[*]*Corresponding author: john.sheridan@ucd.ie*

Received March 30, 2009; revised June 22, 2009; accepted June 22, 2009; posted June 30, 2009 (Doc. ID 109400); published July 29, 2009

Correlation properties of speckle fields at the output of quadratic phase systems with hard square and circular apertures are examined. Using the linear canonical transform and *ABCD* ray matrix techniques to describe these general optical systems, we first derive analytical formulas for determining axial and lateral speckle sizes. Then using a numerical technique, we extend the analysis so that the correlation properties of nonaxial speckles can also be considered. Using some simple optical systems as examples, we demonstrate how this approach may be conveniently applied. The results of this analysis apply broadly both to the design of metrology systems and to speckle control schemes. © 2009 Optical Society of America

OCIS codes: 070.2580, 030.6140, 110.6150.

1. INTRODUCTION

Coherent laser light reflected from an optically rough surface produces a grainy interference pattern known as speckle. For a given illumination wavelength and optical system, this speckle pattern is dependent on the profile of the rough surface. Measuring variations in the speckle field (for example, by capturing a series of sequential images) the user has a noncontact means of monitoring surface changes as external forces and stresses are applied [1–6]. Speckle size plays a role in determining the resolution and dynamic range of such metrology systems, and the ability to predict and control speckle size can thus be used to improve system performance. In speckle photography systems, for example, it can be used to match the speckle and camera pixel sizes, while for speckle interferometry it is preferable to have many speckles per camera pixel [7]. In other optical applications such as digital holography, speckle is treated as a source of noise, and insight into speckle correlation properties may aid in the development of speckle reduction techniques [8]. It is known that speckle size depends on the lenses, apertures, and sections of free space in an optical system. It is also dependent on the wavelength used and, although not discussed here, polarization diversity [8]. In this paper, simple formulas are presented to estimate the lateral and on-axis longitudinal speckle size (for input circular and square hard apertures) at the output of quadratic phase systems described using the linear canonical transform (LCT) and the corresponding ray-tracing *ABCD* matrices [9–11]. The analysis is then extended so that the off-axis speckle sizes can also be determined in a straightforward manner, using a set of simple analytical functions.

Lateral speckle size was first investigated by Goldfisher [12] by examining the width of the autocorrelation function of a free space speckle pattern. Later, Leushacke and Kirchner [13] derived expressions for the average speckle width and length following free space (Fresnel) propagation from both circular and square apertures. On-axis speckle size in general *ABCD* systems with soft Gaussian apodized apertures has been discussed by Yura *et al.* [14]. We have previously determined speckle size numerically in *ABCD* systems for a 1-D rectangular slit [15]; however, these results are somewhat awkward to apply. This paper makes the following additional contributions: (i) The previous analysis [15] is extended to include square and circular apertures; (ii) a set of compact analytical equations that allow straightforward estimation of the lateral and on- and off-axis longitudinal speckle size for any general *ABCD* system is derived, and a simple technique to apply these formulas to system specific solutions is provided; and (iii) some standard optical systems are examined to demonstrate the effectiveness of the resulting approach.

The layout of the paper is as follows: In Section 2 we briefly introduce the LCT and use this transform to describe a speckle field at the output of a general paraxial optical system. This speckle field deforms as optical elements within the bulk optical system are moved or changed. Using correlation techniques we derive a function that provides a measure of the similarity between speckle fields originating from the same input field but propagating through two different LCT systems. We refer to this measure as the mutual correlation coefficient (of intensity) and use it to define speckle size. In Section 3, special cases of the mutual correlation coefficient are examined individually for different input aperture shapes. In Subsection 3.A an expression for the first minimum of the mutual correlation coefficient for 1-D square apertures in generalized *ABCD* systems is derived and is used to define our lateral and on-axis longitudinal speckle

sizes. Subsection 3.B provides a similar analysis for the circular aperture case. In Section 4 the analyses are extended to longitudinal speckle observed off-axis. In Section 5 some commonly used optical systems are examined. Speckle size is calculated for these systems, primarily using the first minimum definition derived in this paper but also using the full-width half-maximum definition sometimes used in the literature [8,11] for the circular aperture case. Finally, in the conclusion in Section 6, a discussion of the main results is presented.

2. *ABCD* RAY MATRICES AND THE CORRELATION COEFFICIENT OF INTENSITY

A. Integral Transforms and the *ABCD* Ray Matrix Notation

Within paraxial scalar diffraction theory, light propagation can be described using the Fresnel transform (FST) and the effect of a thin lens by a chirp transform. All such integral transforms are special cases of the LCT, a three-parameter class of integral transforms that is typically defined in terms of the parameters A, B, and D [5,9–11]. By choosing appropriate values of these parameters, the effect of successive chirp and propagation transforms can be described using the Collins or *ABCD* matrix techniques [9]. The advantage of retaining these A, B, and D parameters throughout a derivation is that the resulting solutions will be applicable to any paraxial quadratic phase system (QPS). In Eq. (1) we define the two-dimensional LCT,

$$\begin{aligned} u(x,y) &= LCT\{u(x_0,y_0)\}(x,y) \\ &= \frac{1}{j\lambda B}\int_{-\infty}^{\infty}\int u(x_0,y_0)p(x_0,y_0) \\ &\quad\times\exp\left[\frac{j\pi}{\lambda B}(Dx^2-2xx_0+Ax_0^2)\right] \\ &\quad\times\exp\left[\frac{j\pi}{\lambda B}(Dy^2-2yy_0+Ay_0^2)\right]\mathrm{d}x_0\mathrm{d}y_0, \end{aligned} \tag{1}$$

where $p(x_0,y_0)$ is the pupil function in the input plane. The 2-D LCT in Eq. (1) describes the mapping of a field $u(x_0,y_0)$, at an optically rough surface, to the field $u(x,y)$ at the output of the LCT system. Equation (2) gives the $[(A,B),(C,D)]$ values in Collins's matrix form [9] for the following: Eq. (2a), propagation through a section of free space or FST; Eq. (2b), a thin lens or chirp modulation; and Eq. (2c), a Fourier transform (FT):

$$\begin{bmatrix} 1 & z \\ 0 & 1 \end{bmatrix}, \tag{2a}$$

$$\begin{bmatrix} 1 & 0 \\ -1/f & 1 \end{bmatrix}, \tag{2b}$$

$$\begin{bmatrix} 0 & 1 \\ -1 & 0 \end{bmatrix}, \tag{2c}$$

where z is the propagation distance, f is the focal length of a convex lens, and the matrices in all the cases we consider have the property $AD-BC=1$. Matrices that describe a combination of the above operations can be constructed by a simple concatenation of the appropriate matrices [5].

B. Mutual Correlation Coefficient of Intensity, μ_I

The mutual correlation coefficient (of intensity) provides a means of comparing the similarity between two fields. It is sometimes referred to in the literature as "the normalised autocorrelation function of intensity" [16], or as "covariance" [6,14], but in all cases represents a normalized form of the correlation between two intensity fields that result from the same input field. The correlation between the light intensity distributions, $I_i(x)=|u_i(x)|^2$ is given by

$$\begin{aligned} &R(x,\tilde{x},ABCD_1,ABCD_2) \\ &\quad=\langle I_{ABCD_1}(x)\rangle\langle I_{ABCD_2}(\tilde{x})\rangle+|J_A(x,\tilde{x},ABCD_1,ABCD_2)|^2, \end{aligned} \tag{3}$$

where $J_A(x,\tilde{x},ABCD_1,ABCD_2)$ is the mutual field amplitude between two Gaussian, statistically independent fields [8,16], captured in different LCT domains and laterally displaced at the output by $\tilde{x}-x$,

$$J_A(x,\tilde{x},ABCD_1,ABCD_2)=\langle u_{ABCD_1}(x)u^*_{\mathrm{ABCD}_2}(\tilde{x})\rangle, \tag{4}$$

where $\langle\cdot\rangle$ denotes ensemble average and subscript $*$ denotes complex conjugation. For notational simplicity in the following expressions, we perform a 1-D analysis. In Section 3 we examine both square and circular apertures and extend the analysis to the 2-D case with appropriate substitutions of variables. Using the 1-D form of Eq. (1), the correlation between two displaced fields in Eq. (4) is given by

$$\begin{aligned} &\left\langle\frac{1}{j\lambda\sqrt{B_1B_2}}\int_{\infty}\int p^2(x_0)u(x_0)u^*(\tilde{x}_0)\right. \\ &\quad\times\exp\left[\frac{j\pi}{\lambda B_1}(D_1x^2-2xx_0+A_1x_0^2)\right], \\ &\quad\left.\times\exp\left[\frac{-j\pi}{\lambda B_2}(D_2\tilde{x}^2-2\tilde{x}\tilde{x}_0+A_2\tilde{x}_0^2)\right]\mathrm{d}x_0\mathrm{d}\tilde{x}_0\right\rangle, \end{aligned} \tag{5}$$

where the pupil function $p(x_0)$ is assumed to be a real-valued, hard-edged aperture at the input plane. We now make two simplifying assumptions about the statistics of the speckle: (i) the speckle field is fully developed and is delta correlated at the rough surface, i.e., $\langle u(x_0)u^*(\tilde{x}_0)\rangle = C\delta(x_0-\tilde{x}_0)$, where C is a constant; and (ii) the intensity fields $\langle I(x)\rangle$ and $\langle I(\tilde{x})\rangle$ are slowly changing and approximately equal to each other [8]. Thus a study of $J_A(x,\tilde{x},z,\tilde{z})$ is sufficient to describe the decorrelation of the speckle field and so the speckle size [13]. We note that if assumption (i) is not satisfied, the following equations are valid only in the far field of the aperture [8] Chap. 4.

Using these assumptions, Eq. (5) can be rewritten as

$$\frac{C\exp\left[\frac{j\pi}{\lambda}\left(\frac{D_1}{B_1}x^2-\frac{D_2}{B_2}\tilde{x}^2\right)\right]}{j\lambda\sqrt{B_1B_2}}\int_{-\infty}^{\infty}p^2(x_0)\times\exp\left\{\frac{j\pi}{\lambda}\left[\left(\frac{\tilde{x}}{B_2}-\frac{x}{B_1}\right)2x_0+\left(\frac{A_1}{B_1}-\frac{A_2}{B_2}\right)x_0^2\right]\right\}\mathrm{d}x_0. \tag{6}$$

The mutual correlation coefficient (of intensity) is equal to the absolute value squared of the normalized mutual field amplitude,

$$\mu_I(x,\tilde{x},ABCD_1,ABCD_2)=\left|\frac{J_A(x,\tilde{x},ABCD_1,ABCD_2)}{\sqrt{J_A(x,x,ABCD_1,ABCD_1)J_A(\tilde{x},\tilde{x},ABCD_2,ABCD_2)}}\right|^2. \tag{7}$$

Substituting Eq. (6) into Eq. (7) gives

$$\left|\frac{\int_{=\infty}^{\infty}p^2(x_0)\exp[j(\alpha x_0+\tau x_0^2)]\mathrm{d}x_0}{\int_{=\infty}^{\infty}p^2(x_0)\mathrm{d}x_0}\right|^2, \tag{8}$$

where

$$\alpha=\frac{2\pi}{\lambda}\left(\frac{\tilde{x}}{B_2}-\frac{x}{B_1}\right),\qquad \tau=\frac{\pi}{\lambda}\left(\frac{A_1}{B_1}-\frac{A_2}{B_2}\right).$$

Equation (8) is the general form of the mutual correlation coefficient used in this paper to derive speckle size for 1-D square aperture systems.

3. LATERAL AND ON-AXIS LONGITUDINAL SPECKLE SIZE

The speckle size for two special and important cases, *lateral* and on-axis *longitudinal* speckles, are now derived. The term lateral refers to speckle width perpendicular to the optical axis, while longitudinal speckle collectively describes speckle length coincident (on-axis) and noncoincident (off-axis) with the optical axis. Mathematical definitions of lateral and longitudinal speckle are used, which allows analytical solutions of Eq. (8) to be found for both aperture types. For lateral speckle we assume that the bulk optical LCT system remains physically unchanged, i.e., $ABCD_1=ABCD_2$; thus $\tau=0$, and Eq. (8) is simplified accordingly. This corresponds to performing an autocorrelation of the speckle intensity pattern and noting the width of the resulting autocorrelation peak. Finding the lateral speckle size thus involves answering the question, how far must we displace the speckle pattern laterally before the first minimum of correlation occurs? In deriving longitudinal speckle size, we examine the decorrelation between two speckle fields produced from the same input field as the *ABCD* system parameters are varied. For the longitudinal case, $ABCD_1\neq ABCD_2$, however, the output planes are assumed laterally stationary, e.g., $x=\tilde{x}$. Furthermore, for *on-axis* longitudinal speckle, $x=\tilde{x}=0$. However this simplification will not be made until the end of the derivations so that off-axis solutions to the mutual correlation coefficient can be explored. The analysis is first performed for 1-D input square apertures and then for 2-D circular apertures.

A. Speckle Size for Square Apertures

The 1-D real-valued pupil function for a hard-edged square aperture is

$$p(x_0)=\begin{cases}1 & |x_0|\leq L/2\\ 0, & \text{otherwise}\end{cases}, \tag{9}$$

where L is the width of the aperture. The full 2-D solution for the square aperture case involves only a multiplication of the two orthogonal 1-D solutions. Equation (8) now becomes

$$\mu_I(x,\tilde{x},ABCD_1,ABCD_2)=\left|\frac{1}{L}\int_{-L/2}^{L/2}\exp[j(\alpha x_0+\tau x_0^2)]\mathrm{d}x_0\right|^2. \tag{10}$$

1. Lateral Speckle Size

Lateral speckle size (speckle width) is defined by the maximum lateral displacement, $\tilde{x}=x$, that can take place before the first minimum of μ_I is reached. Since only an autocorrelation of the field must be considered, $ABCD_1=ABCD_2$ and $\tau=0$. Simplifying Eq. (10) gives

$$\mu_I(x,\tilde{x})=\left|\frac{1}{L}\int_{-L/2}^{L/2}\exp(j\alpha x_0)\mathrm{d}x_0\right|^2=\left|\frac{2\sin\left(\frac{L\alpha}{2}\right)}{L\alpha}\right|^2. \tag{11}$$

The minima of Eq. (11) are located at the points at which $\sin(L\alpha/2)=0$, i.e., when $L\alpha/2=N\pi$, where N is an odd natural number. The first minimum of the correlation coefficient of intensity occurs when $N=1$, giving

$$\frac{L}{2}\frac{2\pi}{\lambda B}(\tilde{x}-x)=\pi. \tag{12}$$

Thus speckle width, ϵ_x, is defined as

$$\epsilon_x=\tilde{x}-x=\lambda B/L. \tag{13}$$

Equation (13) is the general form for speckle width when a square aperture is at the input plane of the system, and B is dependent on the specific parameters of the optical system.

2. Longitudinal Speckle Size

Longitudinal speckle size is defined by the maximum change to the optical system that can take place before the first minimum of μ_I is reached. The lateral position remains unchanged for this case; consequently, $\tilde{x}=x$ and μ_I is no longer a function of lateral displacement. In order to find an analytical solution to Eq. (10), we apply a change of variable, $t=x_0\sqrt{2\tau/\pi}+\alpha/\sqrt{2\tau\pi}$, giving

$$\mu_I(ABCD_1,ABCD_2) = \left| \frac{1}{L}\sqrt{\frac{\pi}{2\tau}}\exp\left[-j\left(\frac{\alpha^2}{4\tau}\right)\right] \times \int_{\alpha/\sqrt{2\tau\pi}-L\sqrt{\pi/2\pi}}^{\alpha/\sqrt{2\tau\pi}+L\sqrt{\pi/2\pi}} \exp\left(\frac{j\pi t^2}{2}\right)\mathrm{d}t \right|^2. \tag{14}$$

Introducing the Fresnel integrals, $C(z)$ and $S(z)$ [13,18], Eq. (14) can be written as

$$\left|\frac{1}{2b}\exp\left[-j\left(\frac{\pi a^2}{2}\right)\right][C(a+b)-C(a-b) + jS(a+b)-jS(a-b)]\right|^2, \tag{15}$$

where $a=\alpha/\sqrt{2\tau\pi}$ and $b=L\sqrt{\tau/2\pi}$. This simplifies to

$$\frac{1}{|2b|^2}\{[C(a+b)-C(a-b)]^2+[S(a+b)-S(a-b)]^2\}. \tag{16}$$

Equation (16) is the general analytical form of $\mu_I(ABCD_1,ABCD_2)$ for longitudinal speckle in a 1-D square aperture system.

For the special case of on-axis speckle, $x=0\Rightarrow a=\alpha=0$, and Eq. (16) can be written as

$$\frac{C^2(b)+S^2(b)}{|b^2|}, \tag{17}$$

since $C(-b)=-C(b)$ and $S(-b)=-S(b)$. The first minimum of Eq. (17) occurs at $b_{\min}=1.9115$. Substituting for b gives $L\sqrt{\tau/2\pi}=1.9115$. Therefore, the first minimum of the mutual correlation coefficient for on-axis longitudinal speckle occurs when

$$\frac{A_1}{B_1}-\frac{A_2}{B_2}=\frac{7.31\lambda}{L^2}. \tag{18}$$

On-axis speckle length is determined from Eq. (18) by substituting in system-specific values of A_1, A_2, B_1, and B_2. The application of Eq. (18) to some well-known optical systems is discussed in Section 5.

B. Speckle Size for Circular Apertures

In this case the 2-D pupil function is given by

$$p(r_0)=\begin{cases}1, & |r_0|\le D_0/2\\ 0, & \text{otherwise}\end{cases}, \tag{19}$$

where D_0 is the aperture diameter. The 2-D equivalent of the mutual correlation coefficient is

$$\mu_I(x,\tilde{x},y,\tilde{y},ABCD_1,ABCD_2) = \left|\frac{\int\int_{-\infty}^{\infty} p^2(x_0,y_0)\exp\{j[(\alpha_x x_0+\alpha_y y_0)+\tau(x_0^2+y_0^2)]\}\mathrm{d}x_0\mathrm{d}y_0}{\int\int_{-\infty}^{\infty} p^2(x_0,y_0)e\mathrm{d}x_0\mathrm{d}y_0}\right|^2, \tag{20}$$

where

$$\alpha_x=\frac{2\pi}{\lambda}\left(\frac{\tilde{x}}{B_2}-\frac{x}{B_1}\right), \qquad \alpha_y=\frac{2\pi}{\lambda}\left(\frac{\tilde{y}}{B_2}-\frac{y}{B_1}\right).$$

Transforming to cylindrical coordinates, $x_0=r_0\cos\theta$, $y_0=r_0\sin\theta$, $\alpha_x=\Omega\cos\phi$, and $\alpha_y=\Omega\sin\phi$, where

$$r_0=\sqrt{x_0^2+y_0^2}, \qquad \Omega=\sqrt{\alpha_x^2+\alpha_y^2}=\frac{2\pi}{\lambda}\left(\frac{\tilde{r}}{B_2}-\frac{r}{B_1}\right),$$

Eq. (20) becomes

$$\mu_I(r,\tilde{r},ABCD_1,ABCD_2) = \left|\frac{\int_0^{\infty}\int_0^{2\pi} p^2(r_0)\exp\{j[\Omega r_0(\cos\theta\cos\phi+\sin\theta\sin\phi)+\pi r_0^2]\}r_0\mathrm{d}\theta\mathrm{d}r_0}{\int_0^{\infty}\int_0^{2\pi} p^2(r_0)r_0\mathrm{d}\theta\mathrm{d}r}\right|^2. \tag{21}$$

Employing trigonometric identities and changing the limits based on the definition of the pupil function, Eq. (21) becomes

$$\left| \frac{\int_0^{D_0/2} \int_0^{2\pi} \exp[j\Omega r_0 \cos(\theta - \phi)] \exp[j\pi r_0^2] r_0 \mathrm{d}\theta \mathrm{d}r_0}{\int_0^{D_0/2} \int_0^{2\pi} r_0 \mathrm{d}\theta \mathrm{d}r} \right|^2 . \tag{22}$$

Performing the integral in the denominator and normalizing the radial coordinate, i.e., $r_N = 2r_0/D_0$, Eq. (22) becomes

$$\left| \frac{1}{\pi} \int_0^1 \int_0^{2\pi} \exp\left[j \frac{\Omega D_0 r_N}{2} \cos(\theta - \phi) \right] \times \exp\left[j \frac{\pi D_0^2 r_N^2}{4} \right] r_N \mathrm{d}\theta \mathrm{d}r_N \right|^2 = \left| \int_0^1 J_0(q r_N) \exp[j p r_N^2] r_N \mathrm{d}r_N \right|^2 , \tag{23}$$

where $p = \pi D_0^2/4$, $p = \Omega D_0/2$, and $J_0(x)$ is the zero-order Bessel function [17]. The integral in Eq. (23) is the Fourier–Bessel or Hankel transform.

1. Lateral Speckle Size

Since only an autocorrelation needs to be considered, $ABCD_1 = ABCD_2$ and $p = \tau = 0$. Equation (23) for lateral speckle is written as

$$\mu_I(r, \tilde{r}) = \left| 2 \int_0^1 J_0(q r_N) r_N \mathrm{d}r_N \right|^2 = \left| \frac{2 J_1(q)}{q} \right|^2 , \tag{24}$$

which is the Airy function [17]. The first minimum of this function occurs at $q_{\min} = 3.832$, and since $B_1 = B_2$,

$$\frac{D_0 \pi}{\lambda B} (\tilde{r} - r) = 3.382. \tag{25}$$

Therefore the speckle width ϵ_r is

$$\epsilon_r = \tilde{r} - r = 1.22 \lambda B / D_0. \tag{26}$$

2. Longitudinal Speckle Size

As before, longitudinal speckle size is defined by the maximum change to the optical system that can take place before maximum decorrelation occurs. In this case, $\tilde{r} = r$ and Eq. (23) is in the form of Eq. (20) in [18]. Therefore

$$\mu_I(ABCD_1, ABCD_2) = \left| 2 \exp\left(\frac{jp}{2} \right) \sqrt{\frac{\pi}{p}} \sum_{n=0}^{\infty} (2n+1) \times (-j)^n J_{n+1/2}\left(\frac{p}{2} \right) \frac{J_{2n+1}(q)}{q} \right|^2 . \tag{27}$$

For the case of on-axis speckle, $r = 0 \Rightarrow q = 0$; furthermore, since

$$\lim_{q \to 0} \left[\frac{J_{2n+1}(q)}{q} \right] = \begin{cases} \frac{1}{2}, & n = 0 \\ 0, & n > 0 \end{cases} . \tag{28}$$

Eq. (27) becomes [19]

$$\left| \sqrt{\frac{\pi}{p}} J_{1/2}\left(\frac{p}{2} \right) \right|^2 = \left| \mathrm{sinc}\left(\frac{p}{2} \right) \right|^2 , \tag{29}$$

where $\mathrm{sinc}(x) = \sin(x)/x$. The first minimum of this function occurs when $p_{\min}/2 = \pi$. Backsubstituting for p gives the equation from which the system specific definition of axial speckle size at the output plane can be extracted,

$$\frac{A_1}{B_1} - \frac{A_2}{B_2} = \frac{8\lambda}{D_0^2}. \tag{30}$$

The application of Eq. (30) is discussed in Section 5.

4. OFF-AXIS LONGITUDINAL SPECKLE SIZE

The analysis in Section 3 provides two closed-form equations to estimate longitudinal speckle length. However these formulas are valid only for speckle observed on the principal axis. Off-axis speckles are those observed in any part of the output plane that is noncoincident with the optical axis. Although the difference in size between on- and off-axis speckles is small close to the optical axis [8], speckle length drops off after this central "plateau."

The analytical solutions for speckle size presented in Section 3 were derived for the special cases of $a = 0$ (on-axis speckle with a square aperture) and $q = 0$ (on-axis speckle with a circular aperture). Without these simplifications, it is not, to our knowledge, possible to extend the simple analytical formulation to the off-axis case. It is however possible to *numerically* determine the relationship between a and b (or p and q) at the first minimum of $\mu_1(ABCD_1, ABCD_2)$. We proceed, following [15], by identifying numerically a "boundary of correlation" (BOC) curve on a contour plot of $\mu_1(ABCD_1, ABCD_2)$. The points on this curve represent the first minima of $\mu_1(ABCD_1, ABCD_2)$ for all possible values of a and b (or p and q). We proceed by fitting analytical functions to these BOC points to provide the user with equations that can be used to determine off-axis speckle size for apertured *ABCD* systems. We also include a "half-maximum" line in the contour plot to mark where $\mu_1(ABCD_1, ABCD_2) = 0.5$ for the circular aperture case. Twice the distance of this curve from the origin is sometimes used in the literature to estimate speckle size [8,14,20]. We note that the half-maximum definition of speckle always predicts a smaller size than the corresponding first-minimum prediction [13]. We have also observed that when using the half-maximum definition, the off-axis decorrelation characteristics appear to be consistently underestimated for the longitudinal case.

A. Square Aperture

For the square aperture case, it is easier to first determine the BOC of $\mu_1(ABCD_1, ABCD_2)$ parameterized in terms of α and τ, as shown in [15]. This is because the first minima of $\mu_1(ABCD_1, ABCD_2)$ are sharper and thus more easily located numerically when the function is pa-

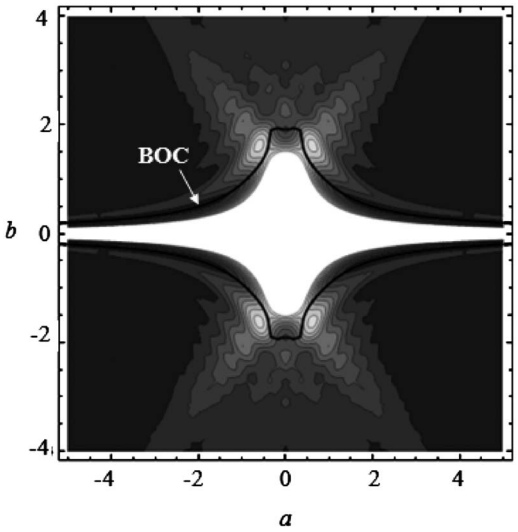

Fig. 1. Contour plot of $\mu_I(ABCD_1,ABCD_2)$ for the square aperture case, where the BOC marks the location of the first minima parameterized in terms of a and b.

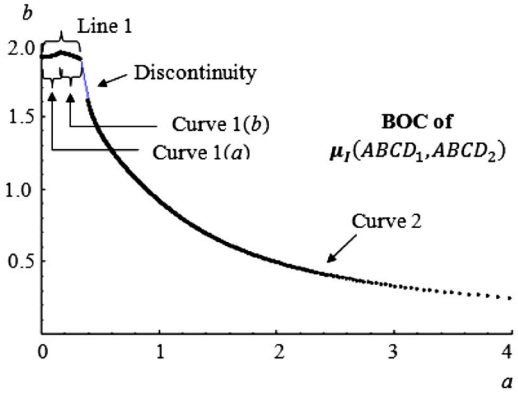

Fig. 2. (Color online) Plot of the BOC for the square aperture case, showing the range of a values for which each segment of the BOC curve is valid.

rameterized in terms of these variables. Applying the mappings $a \to \alpha/\sqrt{2\tau\pi}$ and $b \to L\sqrt{\tau/2\pi}$ gives the BOC shown in Fig. 1, where $\mu_1(ABCD_1,ABCD_2)$ is now parameterized as a function of a and b. A difficulty still remains in identifying minima in the range $0.34 \leq |a| \leq 0.4$. Following detailed numerical examination, we have found that in this range, no sharply defined first minima exist. This can be observed as a discontinuity in Fig. 2 in the region of these a values. The resulting gap in the numerically generated data points is fitted with a thin blue line (short vertical segment near top of figure).

In the BOC curve in the positive quadrant of Fig. 1, a relatively flat segment of the BOC is observed, followed by a longer curve of negative curvature. Given the symmetry of the BOC, the curves corresponding to negative a or b values can be related to those in the positive quadrant by a simple change of sign. In Fig. 2, where the different segments of the BOC are identified more clearly, a slight positive inflection in the flat portion of the BOC is observed. We therefore give the option of classifying this segment either as a straight line, "Line 1," or, if a more accurate representation is required, as the combination of two shallow curves, "Curve 1(a)" and "Curve 1(b)." The longer segment of negative curvature will be referred to as "Curve 2." We note that Curve 2 has been extended to provide values in the region of the discontinuity, i.e., where the minima could not be unambigously identified. In Table 1, the equations descibing each of these curve fits, the range of a values over which each fit is valid, and the mean square error between the data and the fits [21] are given.

In order to solve the equations in Table 1, it is necessary to write them as a function of a single variable. From our definitions, a and b written in terms of the $ABCD$ parameters are

$$a = \frac{x\sqrt{2/(\lambda B_1 B_2)}(B_1 - B_2)}{\sqrt{B_2 A_1 - A_2 B_1}}, \tag{31a}$$

$$b = L\sqrt{\frac{1}{2\lambda}\left(\frac{A_1}{B_1} - \frac{A_2}{B_2}\right)}. \tag{31b}$$

By dividing Eq. (31b) by Eq. (31a) it is possible to rewrite b in terms of a. The equations in Table 1 can then be expressed in terms of a alone and solved. While a different a value will result from each equation, the acceptable a value is the one that lies within the range specified for that equation. By substituting the resulting value of a into Eq. (31a), the off-axis speckle size can be calculated. Special cases of a and b for two simple optical systems are provided in Table 2. In the examples that are provided, Δz refers to an ouput plane normal displacement and will provide a result equivalent to the longitudinal speckle size, ϵ_z, when the a or b values that result from these equations lie on the BOC. In order to simplify the expressions in Table 2, the assumption that $z \gg \Delta z$ was made. Thus for the Fresnel case shown in Fig. 3(a), $z(z+\Delta z) \cong z^2$, and for the single-lens case in Fig. 3(b),

Table 1. Equations Describing the Fits to the Various Segments of the BOC, with the Associated Ranges and Mean-Square-Error Values

Square Aperture	Equation: $b(a)$=	Valid Ranges of a	Mean Square Error [21]
Curve 1	1.911	$0 \leq a \leq 0.337$	2.814×10^{-4}
Curve 1(a)	$1.907+0.004\exp(43.748a^{1.693})$	$0 \leq a \leq 0.163$	5.173×10^{-9}
Curve 1(b)	$1.954\exp(-0.261a^{2.003})$	$0.163 \leq a \leq 0.337$	7.073×10^{-10}
Curve 2	$0.086+3.533\exp(-1.448a^{0.557})$	$0.337 \leq a \leq \infty$	1.409×10^{-4}

Table 2. *a* and *b* Values for Some Commonly Used Optical Systems That Are Laterally Stationary[a]

Square Aperture	a	b	b/a	ϵ_z
FST system	$-x\sqrt{\frac{2\Delta z}{\lambda z^2}}$	$L\sqrt{\frac{\Delta z}{2\lambda z^2}}$	$\frac{-L}{2x}$	$2b_{\min}^2\lambda\left(\frac{z}{L}\right)^2$
Single lens system	$-\sqrt{\frac{2\Delta z}{\lambda}}\frac{x(f_1-z_1)}{[f(z_1+z_2)-z_1z_2]}$	$\sqrt{\frac{\Delta z}{2\lambda}}\frac{fL}{[f(z_1+z_2)-z_1z_2]}$	$-\frac{Lf}{2x(f-z_1)}$	$2b_{\min}^2\lambda\frac{[f(z_1+z_2)-z_1z_2]^2}{fL}$

[a]i.e. $\tilde{x}=x$, where ϵ_z is the corresponding off-axis longitudinal speckle size.

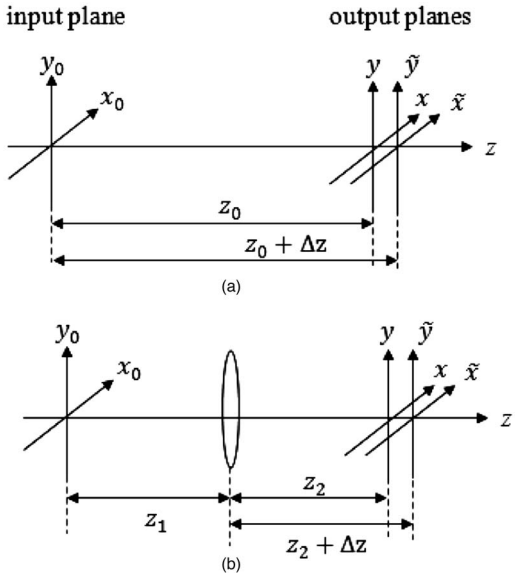

Fig. 3. Schematic representation of (a) a free space optical system, (b) a single-lens system.

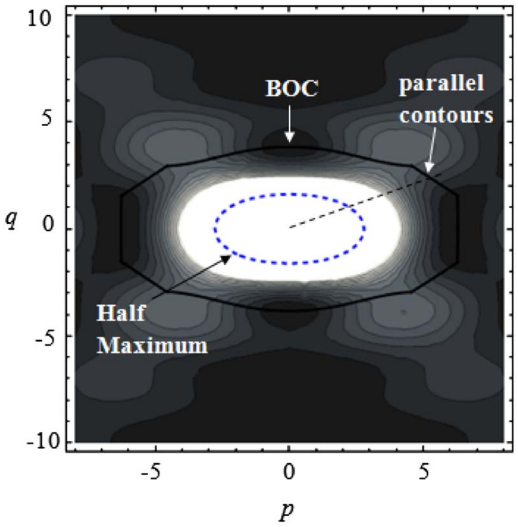

Fig. 4. (Color online) Contour plot of $\mu_I(ABCD_1,ABCD_2)$ parameterized in terms of p and q, showing the BOC for the circular aperture case. Dashes in an oval mark the half-maximum contour.

$fz_2 \cong f(z_2+\Delta z)$. In Section 5, the procedure used to calculate off-axis speckle size for these systems is applied.

B. Circular Aperture

The contour plot of $\mu_1(ABCD_1,ABCD_2)$, parameterized as a function of p and q, is shown in Fig. 4. Using numerical fitting techniques, equations for the three segments of the BOC curve and the half-maximum curve highlighted in Fig. 5 were determined. The equations for the three segments provide the relationship between p and q at the first minima of $\mu_1(ABCD_1,ABCD_2)$ for the ranges and with the accuracies shown. A difficulty arises in identifying minima in the range $5.1 \leqslant p \leqslant 6.55$. Following detailed numerical examination, we have found that in this range no sharply defined first minima exist. This introduces an ambiguity regarding the location of the BOC that can be observed graphically by noting the dashed lines in Fig. 5 or the minima that lie parallel to the contours of $\mu_1(ABCD_1,ABCD_2)$ in Fig. 4. To overcome this ambiguity, we define a straight line to approximate the BOC in this region, going from the minimum q value of Curve 1 to the minimum p value of Curve 2. We refer to this line as the effective BOC line. Table 3 lists the equation describing each curve, the range of p values, and the accuracy of each fit. For completeness, curve fits to the half-maximum contour line are also given. From our definitions, the general expressions for p and q in terms of the $ABCD$ parameters are

$$p = \frac{D_0^2\pi}{4\lambda}\left(\frac{A_2}{B_2}-\frac{A_1}{B_1}\right), \tag{32a}$$

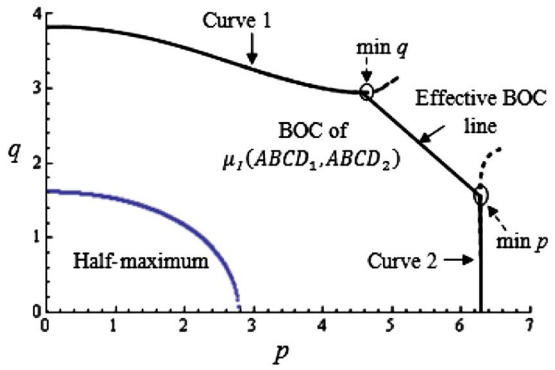

Fig. 5. (Color online) BOC for the circular aperture case, showing the range of p values for which each segment of the BOC is valid.

Table 3. Equations Describing the Fits to the Various Segments of the BOC, with the Associated Ranges and Mean-Square-Error Values for the Circular Aperture Case

Circular Aperture	Equation: $q(p)$	Valid Ranges of p	Mean Square Error [21]
Curve 1	$(1.819\times10^{-5})p^6+(1.327\times10^{-3})p^4-0.078p^2+3.836$	$0\leq p\leq 4.563$	2.619×10^{-5}
Effective BOC line	$-0.813p+6.6558$	$4.563\leq p\leq 6.271$	n/a
Curve 2	$7.77\left[1-\left(\frac{p}{6.283}\right)^2\right]^{0.3}$	$6.271\leq p\leq 6.283$	3.633×10^{-4}
Half-Maximum	$1.6163\left[1-\left(\frac{p}{2.79}\right)^{2.187}\right]^{0.5}$	$0\leq p\leq 2.79$	8.543×10^{-6}

Table 4. p and q Values for Some Commonly Used Optical Systems That Are Laterally Stationary[a]

Circular Aperture	p	q	q/p	ϵ_z
FST system	$\frac{D_0^2\pi\Delta z}{4\lambda}\left(\frac{1}{z^2}\right)$	$\frac{D_0\pi r\Delta z}{\lambda}\left(\frac{1}{z^2}\right)$	$\frac{4r}{D_0}$	$\frac{4p_{\min}\lambda}{\pi}\left(\frac{z}{D_0}\right)^2$
Single lens system	$\frac{D_0^2f^2\pi\Delta z}{4\lambda[f(z_1+z_2)-z_1z_2]^2}$	$\frac{D_0f\pi r(z_1-f)\Delta z}{\lambda[f(z_1+z_2)-z_1z_2]^2}$	$\frac{4r(z_1-f)}{D_0f}$	$\frac{4p_{\min}\lambda}{\pi}\left[\frac{f(z_1+z_2)-z_1z_2}{D_0f}\right]^2$

[a] i.e., $\tilde{r}=r$, where ϵ_z is the corresponding off-axis longitudinal speckle size.

$$q=\frac{D_0\pi r}{\lambda}\left(\frac{1}{B_2}-\frac{1}{B_1}\right). \tag{32b}$$

To extract speckle size information using the functions in Table 1, q is expressed in terms of p, and the equations in Table 3 are solved to find p. The correct p value must lie within the range specified for that equation. By substituting this value of p into Eq. (32a), off-axis speckle size can be found. The p and q values for some well-known optical systems are provided in Table 4. In Section 5, our procedure is applied to analyze these systems assuming input circular apertures.

5. EXAMPLES OF SOME WELL-KNOWN OPTICAL SYSTEMS

Two specific optical configurations are examined: a free space configuration, Fig. 3(a) and a single-lens system, Fig. 3(b). We determine the lateral and on-axis longitudinal speckle size for both cases and examine the change in longitudinal speckle size for a given offset from the optical axis. We note that although only the effect of changing the position of the output plane is examined, the analysis presented is sufficiently general so as to allow one to determine the correlation properties of a speckle system in which any paraxial system component value, i.e., *ABCD* parameter, is changed.

A. Free-Space Propagation (FST)

From Eq. (2), the *ABCD* parameters that describe the Fresnel-transforming systems shown in Fig. 3(a) before displacement of the output plane are $ABCD_1$=Eq. (2a), and following displacement,

$$\begin{bmatrix} A_2 & B_2 \\ C_2 & D_2 \end{bmatrix}=\begin{bmatrix} 1 & z+\Delta z \\ 0 & 1 \end{bmatrix}. \tag{33}$$

1. Square Aperture Case (FST)

Substituting the B values in Eq. (33) into Eq. (13) gives the following expression for the lateral speckle size (speckle width):

$$\epsilon_x=\lambda z/L. \tag{34}$$

The corresponding expression describing on-axis longitudinal speckle size can be found by substituting the above *ABCD* values into Eq. (18), giving

$$\frac{\Delta z}{z(z+\Delta z)}=\frac{7.31\lambda}{L^2}. \tag{35}$$

Assuming that $z\gg\Delta z$, the on-axis longitudinal speckle size ϵ_z is given by

$$\epsilon_z=\Delta z=7.31\lambda(z/L)^2. \tag{36}$$

Both Eqs. (34) and (36) agree with the results in the literature [13]. Using the example of an optical system with z=20 cm, L=10 cm, and λ=633 nm, the speckle width at the output of the system is ϵ_x=1.266 μm, while the on-axis longitudinal speckle size is ϵ_z=18.5 μm.

We now examine the change in longitudinal speckle size for speckles observed off-axis. We use the same system component values as above but now consider $x=-2$ cm in the output plane. For the FST in Table 2, $b=-La/2x$, and the equations in Table 1 can now be written as a function of a only and solved numerically. The a value resulting from Curve 2 is 0.541, which is within the

specified range, i.e., $0.390 \leqslant a \leqslant \infty$. Substituting into $a = -x\sqrt{2\Delta z/\lambda z^2}$ from Table 2 allows us to solve for Δz at the point of decorrelation. In this case the off-axis lonigtudinal speckle size is $\epsilon_z = 9.263$ μm, which is approximately half that of the predicted on-axis speckle size given above. In Fig. 6 we plot ϵ_z as a function of displacement from the optical axis over the range $0 \leqslant x \leqslant 16$ cm for the square aperture case. The gap in the data points arises due to the discontinuity discussed in Subsection 4.A.

2. Circular Aperture Case (FST)

Substituting the *ABCD* values from Eq. (33) into Eq. (26), the speckle width is

$$\epsilon_r = 1.22\lambda z/D_0. \tag{37}$$

The corresponding expression governing the on-axis longitudinal speckle size, Eq. (30), is

$$\frac{\Delta z}{z(z+\Delta z)} = \frac{8\lambda}{D_0^2}, \tag{38}$$

and therefore ϵ_z is given by

$$\epsilon_z = \Delta z = 8\lambda(z/D_0)^2, \tag{39}$$

in agreement with [13]. For an optical system with $z = 20$ cm, $D_0 = 10$ cm, and $\lambda = 633$ nm, the speckle width at the output of the system is $\epsilon_r = 1.545$ μm, while the on-axis longitudinal speckle size is $\epsilon_z = 20.256$ μm. The equivalent on-axis longitudinal speckle size using the half-maximum definition is $\epsilon_z = 16.96$ μm.

We now examine the change in longitudinal speckle size for speckles observed off-axis at $r = +2$ cm in the output plane. For the FST case in Table 4, $q = 4rp/D_0$. Using this expression, the equations in Table 3 can be written as a function of p only and solved numerically. The p value resulting from Curve 1 is 3.801, which is within the specified range $0 \leqslant p \leqslant 4.563$. Substituting this into $p = [(D_0^2\pi\Delta z)/4\lambda](1/z^2)$ from Table 2, the value of Δz at the point of decorrelation can be found. At $r = 2$ cm from the optical axis, off-axis longitudinal speckle size is $\epsilon_z = 12.254$ μm. In Fig. 7 we plot ϵ_z as a function of displacement from the optical axis over the range $0 \leqslant r \leqslant 16$ cm for this circular aperture case.

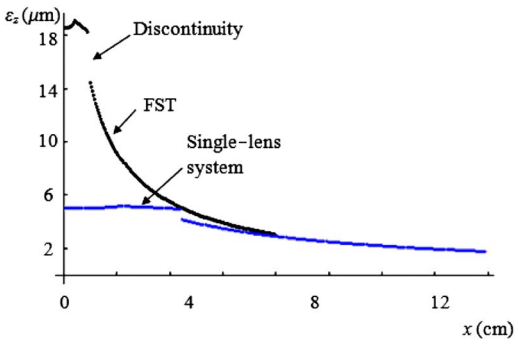

Fig. 6. (Color online) Longitudinal speckle size ϵ_z as a function of displacement x from the optical axis for a square aperture FST and a single-lens system.

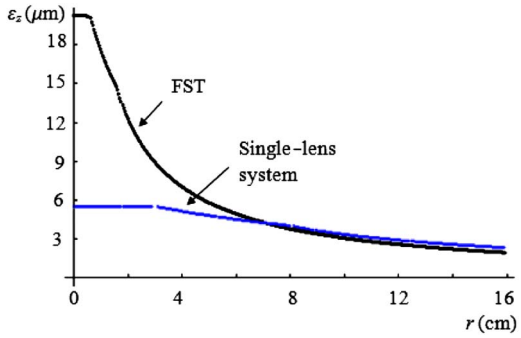

Fig. 7. (Color online) Longitudinal speckle size ϵ_z as a function of displacement r from the optical axis for a circular aperture FST and a single lens optical system.

B. Single-Lens System

Using the matrix concatenation method described in Subsection 2.A, the *ABCD* parameters that describe the single-lens systems in Fig. 3(b) before and after displacement of the output plane are

$$ABCD_1 = \begin{bmatrix} 1 - z_2/f & z_2 + z_1(1 - z_2/f) \\ -1/f & 1 - z_1/f \end{bmatrix}, \tag{40a}$$

and

$$ABCD_2 = \begin{bmatrix} 1 - \dfrac{z_2 + \Delta z}{f} & z_2 + \Delta z + z_1\left(1 - \dfrac{z_2 + \Delta z}{f}\right) \\ -1/f & 1 - z_1/f \end{bmatrix}. \tag{40b}$$

In what follows, we assume $z_1 z_2 \cong z_1(z_2 + \Delta z)$ and $fz_2 \cong f(z_2 + \Delta z)$.

1. Square Aperture Case

In this case the lateral speckle size is given by

$$\epsilon_x = \frac{\lambda}{L}\left[z_2 + z_1\left(1 - \frac{z_2}{f}\right)\right] \tag{41}$$

and on-axis longitudinal speckle size by

$$\epsilon_z = \Delta z = 7.31\lambda\left[\frac{f(z_1 + z_2) - z_1 z_2}{fL}\right]^2. \tag{42}$$

The procedure for determining off-axis speckle size follows that used for the Fresnel system. Figure 6 plots longitudinal speckle size as a function of off-axis displacement x for the square aperture case when $z_1 = 8$ cm, $z_2 = 12$ cm, $L = 10$ cm, and $\lambda = 633$ nm.

2. Circular Aperture Case

For this case the lateral speckle size is given by

$$\epsilon_r = \frac{1.22\lambda}{D_0}\left[z_2 + z_1\left(1 - \frac{z_2}{f}\right)\right] \tag{43}$$

and the on-axis longitudinal speckle size by

$$\epsilon_z = \Delta z = 8\lambda\left[\frac{f(z_1+z_2)-z_1z_2}{D_0 f}\right]^2. \quad (44)$$

In Fig. 7, the longitudinal speckle size is plotted as a function of off-axis displacement r for the circular aperture case when $z_1=8$ cm, $z_2=12$ cm, $D_0=10$ cm, and $\lambda=633$ nm.

6. CONCLUSION

The correlation properties of speckle fields at the output of paraxial optical systems with hard square and circular apertures at the input are examined using the mutual correlation coefficient of intensity. Formulating this correlation method using the linear canonical transform, (LCT) allows us to derive general analytical formulas for lateral and on-axis longitudinal speckle size. A "boundary of correlation" (BOC) curve, defining the first minimum of the mutual correlation coefficient for all cases of longitudinal speckle was generated using a numerical search algorithm. Applying the resulting analytical fits to the various BOC curves, off-axis speckle size can be determined for such systems. Analytical fits to the half-maximum contour are also provided for the circular aperture case. The approach presented provides a general method for calculating speckle decorrelation and thus size in a practical way for a large class of paraxial optical systems.

The results of this paper are of particular significance to any application in which control over speckle size is desirable. The sensitivity and dynamic range of speckle metrology systems, for example, is highly influenced by speckle size. Also, with recent developments in nonimaging speckle photography configurations [3–5], speckle correlation characteristics in generalized optical systems are particularly topical.

Finally, we note that in the derivations presented in this paper, fully developed speckle is assumed, and the correlation extent of the field at the input plane is defined as sufficiently small that it can be adequately represented by a delta function [8]. It is, however, possible that these conditions are only approximately satisfied under certain experimental conditions. In such instances a more involved examination is required; see, for example, Section 4.5 [8]. Experimental verification remains necessary in order to fully assess the validity of the techniques presented. Such a study should indicate the suitability of the first minimum of the correlation coefficient of intensity as the most appropriate method of defining speckle size.

ACKNOWLEDGMENTS

We acknowledge the support of Enterprise Ireland and Science Foundation of Ireland through the Research Innovation Fund and Research Frontiers Programmes, respectively. We also acknowledge the support of the Irish Research Council for Science, Engineering and Technology, and FAS (Training and Employment Authority, Ireland) through the FAS Science Challenge. The research leading to these results has also received funding from the European Community's Seventh Framework Programme FP7/2007-2013 under grant agreement no. 216105

REFERENCES

1. P. K. Rastogi, "Techniques of displacement and deformation Measurements in speckle metrology," in *Speckle Metrology*, R. S. Sirohi, ed. (Marcel Dekker, 1993), pp. xx–xx.
2. H. Tiziani, "A study of the use of laser speckle to measure small tilts of optically rough surfaces accurately," Opt. Commun. **5**, 271–274 (1972).
3. J. T. Sheridan and R. Patten, "Holographic interferometry and the fractional Fourier transformation," Opt. Lett. **25**, 448–450 (2000).
4. D. P. Kelly, B. M. Hennelly, and J. T. Sheridan, "Magnitude and direction of motion with speckle correlation and the optical fractional Fourier transform," Appl. Opt. **44**, 2720–2727 (2005).
5. B. M. Hennelly, D. P. Kelly, J. E. Ward, R. Patten, U. Gopinathan, F. T. O'Neill, and J. T. Sheridan, "Metrology and the linear canonical transform," J. Mod. Opt. **53**, 2167–2186 (2006).
6. T. Fricke-Begemann, "Three-dimensional deformation field measurement with digital speckle correlation," Appl. Opt. **42**, 6783–6796 (2003).
7. T. Yoshimura, M. Zhou, K. Yamahai, and Z. Liyan, "Optimum determination of speckle size to be used in electronic speckle pattern interferometry," Appl. Opt. **34**, 87–91 (1995).
8. J. W. Goodman, *Speckle Phenomena in Optics* (Roberts, 2007).
9. S. A. Collins, Jr., "Lens-system diffraction integral written in terms of matrix optics," J. Opt. Soc. Am. **60**, 1168–1177 (1970).
10. S. Abe and J. T. Sheridan, "Optical operations on wave functions as the Abelian subgroups of the special affine Fourier transformation," Opt. Lett. **9**, 1801–1803 (1994).
11. R. S. Hansen, H. T. Yura, and S. G. Hanson, "First-order speckle statistics: an analytic analysis using *ABCD* matrices," J. Opt. Soc. Am. A **14**, 3093–3098 (1997).
12. L. I. Goldfischer, "Autocorrelation function and power spectral density of laser-produced speckle patterns," J. Opt. Soc. Am. **55**, 247–253 (1965).
13. L. Leushacke and M. Kirchner, "Three-dimensional correlation coefficient of speckle intensity for rectangular and circular apertures," J. Opt. Soc. Am. A **7**, 827–832 (1990).
14. H. T. Yura, S. G. Hanson, R. S. Hansen, and B. Rose, "Three-dimensional speckle dynamics in paraxial optical systems," J. Opt. Soc. Am. A **16**, 1402–1412 (1999).
15. D. P. Kelly, J. E. Ward, U. Gopinathan, and J. T. Sheridan, "Controlling speckle using lenses and free space," Opt. Lett. **32**, 3394–3396 (2007).
16. J. C. Dainty, "The statistics of speckle patterns," in *Progress in Optics, Vol. XIV*, E. Wolf, ed. (North-Holland, Amsterdam, 1976).
17. J. W. Goodman, *Introduction to Fourier Optics*, 3rd ed. (Roberts, 2005).
18. B. R. A. Nijboer, "The diffraction theory of optical aberrations: II. Diffraction pattern in the presence of small aberrations," Physica (Utrecht) **13**, 605–620 (1947).
19. M. Abramowitz and I. A. Stegun, *Handbook of Mathematical Functions* (Dover, 1970).
20. T. Yoshimura and S. Iwamoto, "Dynamic properties of three-dimensional speckles," J. Opt. Soc. Am. A **10**, 324–328 (1993).
21. E. W. Weisstein, "ANOVA," in *MathWorld*, A Wolfram Web Resource; http://mathworld.wolfram.com/ANOVA.html (July 2009).